AIP | Applied Physics Letters

Secondary electron emission from lithium and lithium compounds

A. M. Capece, M. I. Patino, Y. Raitses, and B. E. Koel

Citation: Applied Physics Letters **109**, 011605 (2016); doi: 10.1063/1.4955461
View online: http://dx.doi.org/10.1063/1.4955461
View Table of Contents: http://scitation.aip.org/content/aip/journal/apl/109/1?ver=pdfcov
Published by the AIP Publishing

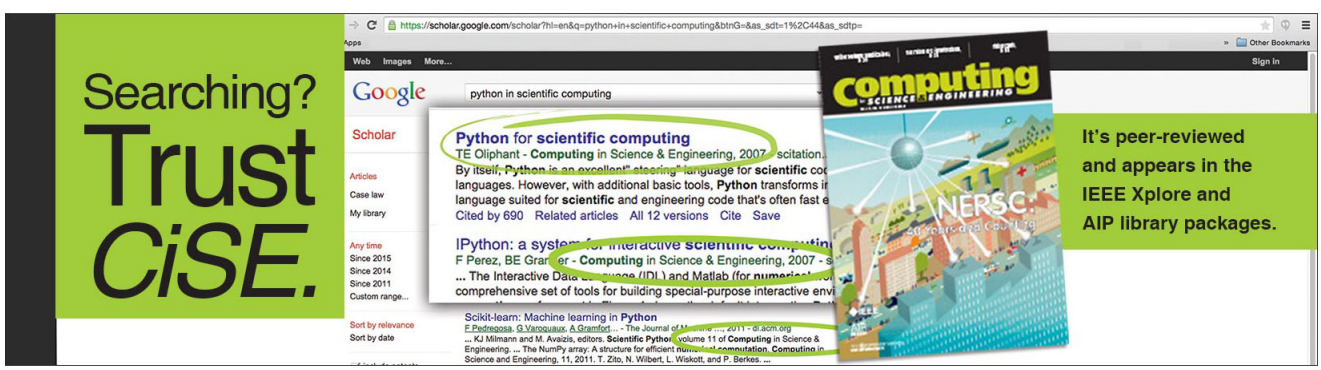

Secondary electron emission from lithium and lithium compounds

A. M. Capece,[1,2,a)] M. I. Patino,[1,b)] Y. Raitses,[1] and B. E. Koel[3]
[1]*Princeton Plasma Physics Laboratory, Princeton, New Jersey 08543, USA*
[2]*Department of Physics, The College of New Jersey, Ewing, New Jersey 08628, USA*
[3]*Department of Chemical and Biological Engineering, Princeton University, Princeton, New Jersey 08540, USA*

(Received 17 March 2016; accepted 25 June 2016; published online 6 July 2016)

In this work, measurements of electron-induced secondary electron emission (SEE) yields of lithium as a function of composition are presented. The results are particularly relevant for magnetic fusion devices such as tokamaks, field-reversed configurations, and stellarators that consider Li as a plasma-facing material for improved plasma confinement. SEE can reduce the sheath potential at the wall and cool electrons at the plasma edge, resulting in large power losses. These effects become significant as the SEE coefficient, γ_e, approaches one, making it imperative to maintain a low yield surface. This work demonstrates that the yield from Li strongly depends on chemical composition and substantially increases after exposure to oxygen and water vapor. The total yield was measured using a retarding field analyzer in ultrahigh vacuum for primary electron energies of 20–600 eV. The effect of Li composition was determined by introducing controlled amounts of O_2 and H_2O vapor while monitoring film composition with Auger electron spectroscopy and temperature programmed desorption. The results show that the energy at which $\gamma_e = 1$ decreases with oxygen content and is 145 eV for a Li film that is 17% oxidized and drops to less than 25 eV for a fully oxidized film. This work has important implications for laboratory plasmas operating under realistic vacuum conditions in which oxidation significantly alters the electron emission properties of Li walls. *Published by AIP Publishing*. [http://dx.doi.org/10.1063/1.4955461]

Electron-induced secondary electron emission (SEE) is the process by which electrons are emitted from a material as a result of ionization and/or excitation of the atoms within the target material by incident electron bombardment or as a result of backscattering of the incident electrons. SEE is important for a variety of applications, including Hall thrusters,[1,2] tokamaks,[3–5] plasma processing devices,[6,7] and particle accelerators.[8,9] Electrons in the plasma with sufficient energy to overcome the sheath potential will impact the surface and cause secondary electrons to be emitted. The emitted electrons are cold, with electron temperatures of a few eV. SEE reduces the sheath potential and cools the electrons at the plasma edge, resulting in large power losses.[10,11]

Assuming the plasma electrons have a Maxwellian velocity distribution with temperature T_e, the sheath potential at the wall drops as the SEE coefficient, γ_e (which includes both true SEE and electron backscatter[10]), increases according to[11]

$$\phi \approx -T_e \ln\left[(1-\gamma_e)\sqrt{\frac{M_i}{2\pi m_e}}\right], \tag{1}$$

where γ_e is defined as the ratio of the emitted electron flux to the primary electron flux. The heat flux density to the wall from the plasma is[11]

$$q = \left(\frac{2kT_e}{1-\gamma_e} - e\phi\right)\Gamma_i, \tag{2}$$

where Γ_i is the ion flux to the surface. It follows from Eqs. (1) and (2) that as γ_e approaches one, the power losses become large. This is problematic for all plasma devices, and therefore, it is crucial that the SEE coefficient remains below one.

One candidate for the plasma-facing material in advanced divertor concepts for magnetic fusion devices is lithium, which has a maximum SEE coefficient of 0.56 when metallic.[12] Lithium effectively traps and retains hydrogen ions that escape the fusion plasma, which results in a low recycling wall and has led to improved plasma performance on a variety of fusion devices.[13] Although the SEE coefficient for pure Li is below the critical value of one for all incident electron energies, the SEE coefficient exceeds one for incident electron energies as low as 20 eV when Li is oxidized.[12]

Li is very reactive, and recent surface science experiments show that a Li film 5 nm thick will be completely oxidized after exposure to 20–40 L (1 L = 1×10^{-6} Torr s) of O_2 or water vapor.[14] That is, a 5 nm thick Li film will be oxidized in 20–40 s at a water partial pressure of 10^{-6} Torr. Such exposures are common in fusion devices, which have pressures of 10^{-6} to 10^{-5} Torr between plasma shots. Therefore, it is unrealistic to expect pure Li walls to exist at the plasma boundary in these devices. It is imperative that Li walls be considered as a mixed material containing both Li metal and Li oxide.

Previous models have predicted that SEE may be suppressed in fusion devices by the magnetic field, which causes emitted electrons to recycle back to the surface via Larmor gyration around magnetic field lines.[15–18] However, Subba *et al.* and Igitkhanov *et al.* model the SEE yield with a

a)Email: capecea@tcnj.edu.
b)Permanent address: Department of Mechanical and Aerospace Engineering, University of California, Los Angeles, California 90095, USA.

maximum value less than or equal to one because it is characteristic of graphite.[16,17] Given that yields for realistic Li surfaces may exceed one at low primary electron energies, it is important to reconsider these results for wall materials with larger yields. In their model, Mizoshita *et al*. consider a fixed electric field at the wall without accounting for the effects of SEE on the sheath, and they do not consider primary electrons at grazing incidence, which will enhance the yield.[18]

SEE yields of Li were measured by Bruining and de Boer for pure and impure Li surfaces at electron energies ranging from 20 to 900 eV (Ref. 12) and inferred by Oyarzabal *et al*. from *I-V* curves of a Li target immersed in He and Ar plasmas for energies up to 120 eV.[19,20] The surface composition was not measured in either study, and no data exist on the impurity level of these surfaces. However, the yield results varied considerably between the "pure" and "impure" surfaces. For example, the maximum yields were measured as 0.56 and 4.2 for pure and impure Li, respectively.[12] These results represent the lower and upper bounds of SEE coefficients for Li; however, no results of realistic Li surfaces containing a mixture of Li metal and oxide are available to date. In this work, total electron yields (TEY) of different Li surfaces are measured for primary electron energies of 25–600 eV.

In order to measure the yield as a function of composition, it is necessary to perform *in situ* measurements of the surface during yield measurements. This was achieved in this work by conducting experiments in an ultrahigh vacuum (UHV) chamber equipped with Auger electron spectroscopy (AES) for surface compositional analysis and a retarding field analyzer for yield measurements. The effect of Li composition on total electron yield was determined by introducing controlled amounts of O_2 and H_2O vapor.

Experiments were performed at the Princeton Plasma Physics Laboratory in a stainless steel UHV chamber with a base pressure of 5×10^{-10} Torr pumped by a 170 l/s turbomolecular pump and 440 l/s ion pump. The chamber was equipped with a Physical Electronics, Inc. (PHI) model 255G cylindrical mirror analyzer for AES, PHI model 15–120 low energy electron diffraction (LEED) optics, a tectra GenII electron cyclotron resonance (ECR) plasma source, and a UTI 100C quadrupole mass spectrometer (QMS) used for temperature programmed desorption (TPD) studies. A Ni(110) single crystal polished to a surface roughness of less than 0.01 μm was used as the substrate material. The Ni sample was mounted between two Ta posts by spotwelding to 0.015-in. diameter Ta wires. The sample was sputter cleaned with 1-keV Ar^+ ions from the ECR plasma source to remove sulfur impurities, and cleaned of oxygen and carbon contamination by flashing to 1150 K.

Lithium was deposited onto the Ni sample by thermal evaporation from a SAES Getters alkali metal dispenser while the sample was held at room temperature.[21] The Li film thickness in our experiments was determined using TPD, which was conducted by resistively heating the sample with a 7–10 K/s linear temperature ramp up to 1300 K while monitoring the Li ($m/q = 7$) signal with the QMS while the sample was in direct line of sight of the ionizer. Temperature control was implemented using a Eurotherm 3508 PID controller, and temperature was monitored using a type C thermocouple spot-welded to the back of the Ni sample. The film thickness was calculated by comparing the total area under the Li desorption curve to the integral of the Li monolayer desorption curve.[22] The amount of Li measured was converted to a film thickness assuming the metallic radius of Li is 1.52 Å (Ref. 23) and the lattice parameter of Li_2O is 4.62 Å.[24] Results are shown in Fig. 1 for a 25-nm Li film on Ni(110). The low temperature peak, at 600 K for this Li coverage, represents desorption of Li from a multilayer Li film.[22] The peaks at 770 and 910 K correspond to the decomposition and desorption of Li oxide.[25]

The films studied here include Li oxide films 10 nm thick and mixed films of Li metal and Li oxide 25 nm thick. It is known that surface roughness affects TEY; however, the effects have been shown to be negligible for a surface roughness of less than 100 nm.[26] Given that the roughness of the Ni substrate in this work is less than 10 nm and the Li films are 10–25 nm thick, the roughness of these Li surfaces is much less than 100 nm. Additionally, the Li films appear continuous as evidenced by the absence of Ni peaks in the AES spectra shown in Fig. 4. The effects of surface roughness on the TEY measurements presented here are therefore negligible.

The penetration depths of electrons in these films were determined using CASINO v2.48, a publicly available program based on the Monte Carlo method,[27] to ensure that there are no contributions to the yield from the Ni substrate. The most probable depth for 600 eV electrons in pure Li is 39 nm and the maximum penetration depth is 56 nm. In Li_2O, the most probable penetration depth of 600 eV electrons is 10 nm and the maximum depth is 17 nm. For mixed films, assuming a 5-nm thick film of Li_2O on Li, the most probable and maximum penetration depths of 600 eV electrons are 25 and 40 nm, respectively. The film thicknesses used in this work are close to these calculated penetrations depths; however, the region of interest in this work is where the yield approaches the critical value of $\gamma_e = 1$, which

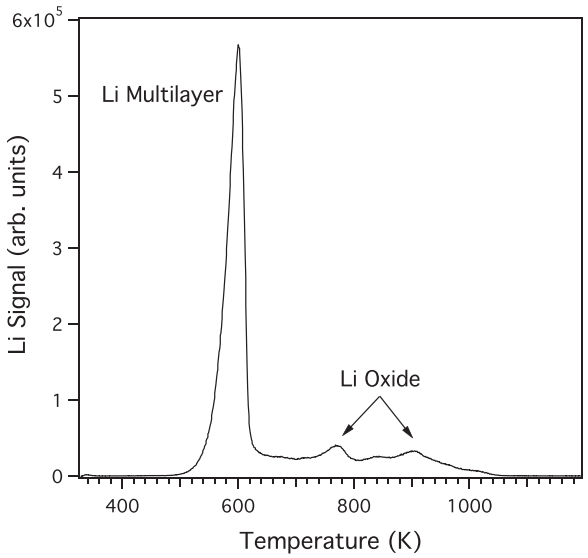

FIG. 1. TPD trace from a 25-nm Li film on Ni(110). Desorption of the multilayer starts at 500 K, and decomposition and desorption of Li oxide occurs at 770 and 910 K.

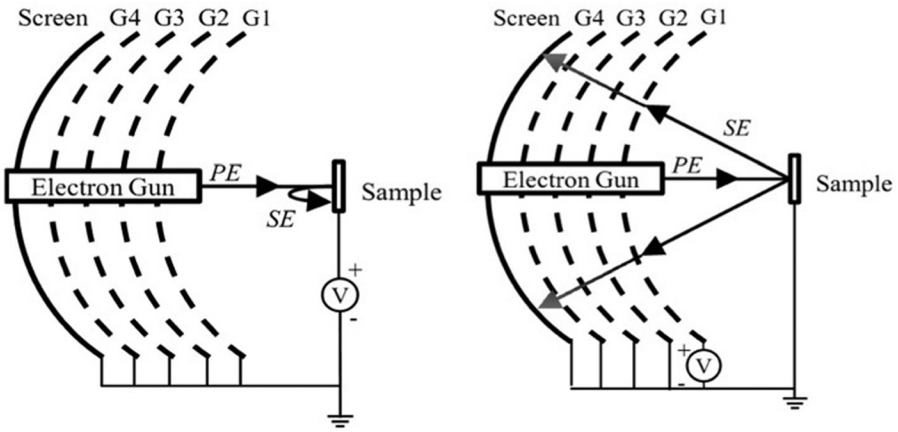

FIG. 2. Sample and LEED optics when measuring primary electron current (left) and secondary electron current (right).

occurs at low energies (less than 200 eV). The maximum penetration depth for 200 eV electrons in Li films is 8 nm, and therefore, the films generated in this work are thick enough to provide reliable yield data at low energies near the critical yield of $\gamma_e = 1$.

Total electron yield was measured with the LEED optics, which contains an electron gun used to produce primary electrons with energies up to 600 eV. The primary electron current, I_{PE}, was measured by biasing the sample to between +50 and +150 V to suppress SEE. The SEE current, I_{SE} (which includes both secondary and backscattered electrons), was measured with the sample at room temperature using two methods for improved accuracy:[3,28–30] (1) sample method and (2) collector method. In the sample method, the current measured on the sample when grounded or biased slightly negative (i.e., to −20 V), I_s, is due to incident primary electrons and emitted secondary electrons such that $I_s = I_{PE} - I_{SE}$. The total electron yield is then

$$\gamma_e = \frac{I_{SE}}{I_{PE}} = \frac{I_{PE} - I_s}{I_{PE}} = 1 - \frac{I_s}{I_{PE}}. \quad (3)$$

In the collector method, the surfaces of the LEED optics (i.e., hemispherical concentric grids and a final hemispherical screen) collect electrons emitted from the sample such that $I_{LEED} = I_{SE}$ and

$$\gamma_e = \frac{I_{LEED}}{I_{PE}}. \quad (4)$$

To increase collection of electrons beyond the 120° angle of the LEED optics, the first grid, G1 in Fig. 2, was biased to +36 V. A Keithley 2410 sourcemeter was used to bias the sample and measure I_s. A Keithley 6485 picoammeter was used to measure current to the optics.

Figure 3 shows the total electron yield measured using the collector method as a function of primary electron energy for Li films 10–25 nm thick. The results for the sample method are not shown, but are within 10% of the values for the collector method. The experiments were benchmarked against data from Mayer and Weiss[31] for Ni(110) at an angle of 50° (Fig. 3, inset). For fully oxidized Li, two datasets were collected for each film over a 1-h time period and no change in the yields was observed, indicating that charging does not occur for these films. This may be the result of electron tunneling, which can occur in lithium oxide films 5–10 nm thick.[32,33]

Curves (a) and (f) in Fig. 3 represent previous results from Bruining and de Boer[12] for pure and impure Li films, respectively, and are plotted for comparison. Curves (b) and (c) are Li films 23 and 25 nm thick, respectively, that were exposed to an outgassing event during Li deposition that led to some oxidation of the surface. TPD was performed after yield measurements, and the results indicated that both metallic Li and Li oxide were present in the films. The Li/LiO_x ratios in films (b) and (c) were 4.8 and 1.8, respectively (i.e., 17% and 37% of films (b) and (c) were oxidized). TPD results for film (c) are shown in Fig. 1. The yield curves for films (b) and (c) are shifted upward from the measurements by Bruining and de Boer and have maximum yields of 1.1 and 1.4, respectively. Film (b) reaches the critical value of $\gamma_e = 1$ at 145 eV, and film (c) reaches the critical yield at 130 eV. Error bars are shown for curves (b)–(e), which include instrumentation error of the Keithley 2410 sourcemeter and Keithley 6485 picoammeter in addition to systematic error due to nonsaturation of currents when attempting to fully collect or repel secondary electrons.

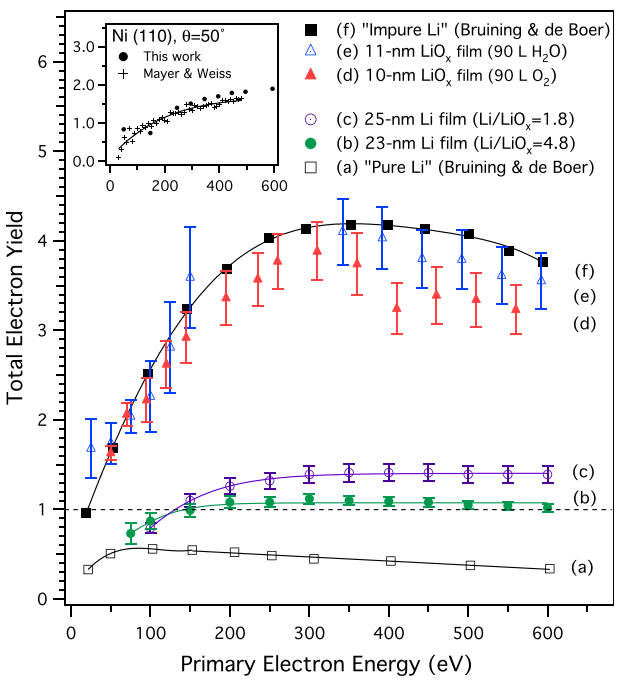

FIG. 3. TEY of Li films 10–25 nm thick. Inset shows TEY for Ni(110) compared with data from Mayer and Weiss.[31]

Curve (d) shows yield results for a 10-nm thick Li film that was oxidized by evaporating Li onto the Ni sample in a background of O_2 gas (99.999%, Specialty Gases of America) at a partial pressure of 1×10^{-7} Torr for 15 min (i.e., 90-L O_2 exposure) while the sample was held at a constant temperature of 300 K. Curve (e) shows results of an 11-nm thick Li film that was oxidized by evaporating Li onto the Ni sample in a background of water vapor (prepared using a freeze-pump-thaw degasification procedure in a Schlenk flask) at a partial pressure of 1×10^{-7} Torr for 15 min (i.e., 90-L H_2O exposure) with the sample held at a temperature between 180 and 200 K. The deposition was performed in this way to ensure complete oxidation of the Li films in order to obtain an upper bound on the total electron yield. The yields of films (d) and (e) match those of Bruining and de Boer[12] for their impure Li film, particularly at low energies (less than 150 eV). The relative error in the yield measurements for film (d) is 5%–10% for all energies, and the relative error for film (e) is 10%–20% for energies less than 200 eV and less than 10% for energies greater than 200 eV.

AES spectra of films (d) and (e) are shown in Fig. 4 along with a pure Li film 30 nm thick for comparison. Some fluorine is present in the AES spectrum for film (d), which may be the result of exposure to an outgassing event by a polytetrafluoroethylene component that occurred prior to yield measurements. Post-experiment TPD measurements of films (d) and (e) indicate full conversion of both films to Li oxide, and no metallic Li was detected. For these fully oxidized films, the critical yield of $\gamma_e = 1$ is reached for electron energies below 25 eV.

Hoenigman and Keil determined by using X-ray photoelectron spectroscopy that a 1-monolayer Li film exposed to between 5 and 100 L of O_2 resulted in the formation of Li_2O.[34] They also suggested that for H_2O exposures between 1 and 100 L, Li_2O is predominant over LiOH at room temperature. Hence, for 1 monolayer of Li and for O_2 and H_2O exposures less than 100 L, O_2 and H_2O are dissociated on Li to form Li_2O. Assuming this to also be true for Li films thicker than 1 monolayer, the similarity in the yield curves between the samples of Li exposed to 90 L of O_2 and 90 L of H_2O can be explained by the formation of Li_2O in both samples.

The results of Fig. 3 indicate that the total electron yield from Li increases after exposure to O_2 and H_2O, and the energy at which $\gamma_e = 1$ decreases with oxygen content. These results are in agreement with Bruining and de Boer,[12] but contradict the conclusions of Oyarzabal *et al.*,[19] which were based on sputter times of oxidized Li immersed in a He plasma. No direct measurements of oxygen contamination in the Li were reported by Oyarzabal, and it is not clear if the He plasma was effective at sputtering the oxygen or if it introduced more impurities due to the high gas pressure. In this work, we presented yield measurements in addition to AES and TPD spectra of oxidized Li films. The lowest yield (with a maximum of 1.1) was measured for a Li film that was 17% oxidized. The energy at which $\gamma_e = 1$ was 145 eV for this film. The highest yield (with a maximum of 4.1) was measured for the fully oxidized film, and the energy at which $\gamma_e = 1$ was less than 25 eV for this film. Therefore, when modeling the plasma–wall interactions in devices with Li walls, it is important to consider the higher yield for oxidized Li presented herein, as this is more representative of the actual Li state in devices with realistic vacuum systems. It is necessary to consider SEE because it can reduce the sheath potential and produce significant power losses for incident electron energies as low as 20 eV.

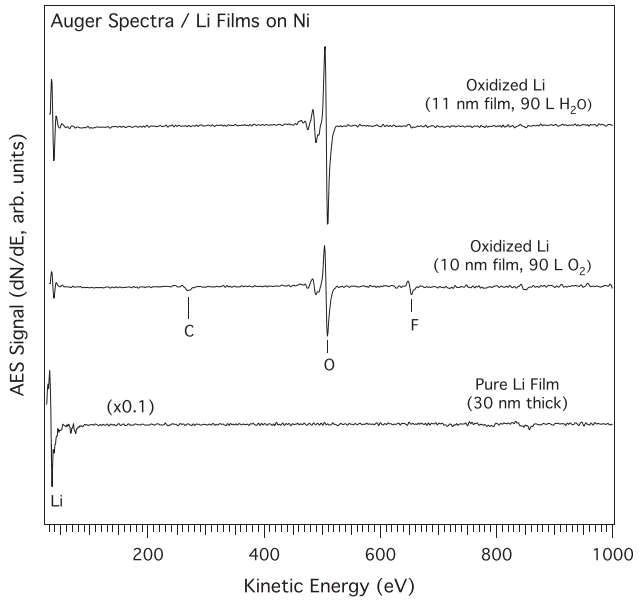

FIG. 4. AES spectra of Li on Ni(110) for different Li films.

The authors would like to thank Alex Merzhevskiy for technical assistance. This work was supported by DOE Contract No. DE-AC02-09CH11466, AFOSR Grant Nos. FA9550-11-1-0282 and AF9550-09-1-0695, and DOE Office of Science Graduate Student Research Program. B. E. Koel acknowledges support of this work by the U.S. Department of Energy, Office of Science/Fusion Energy Sciences, under Award No. DE-SC0012890.

[1]Y. Raitses, I. D. Kaganovich, A. Khrabrov, D. Sydorenko, N. J. Fisch, and A. Smolyakov, IEEE Trans. Plasma Sci. **39**, 995 (2011).
[2]D. Sydorenko, A. Smolyakov, I. Kaganovich, and Y. Raitses, Phys. Plasmas **15**, 053506 (2008).
[3]H. Farhang, E. Napchan, and B. H. Blott, J. Phys. D: Appl. Phys. **26**, 2266 (1993).
[4]J. P. Gunn, Plasma Phys. Controlled Fusion **54**, 085007 (2012).
[5]W. Lee and S. I. Krasheninnikov, Phys. Plasmas **20**, 122501 (2013).
[6]A. J. Perry, D. Vender, and R. W. Boswell, J. Vac. Sci. Technol., B **9**, 310 (1991).
[7]J. Goree, Plasma Sources Sci. Technol. **3**, 400 (1994).
[8]R. Cimino, I. R. Collins, M. A. Furman, M. Pivi, F. Ruggiero, G. Rumolo, and F. Zimmermann, Phys. Rev. Lett. **93**, 014801 (2004).
[9]R. Cimino and T. Demma, Int. J. Mod. Phys. A **29**, 1430023 (2014).
[10]P. C. Stangeby, *The Plasma Boundary of Magnetic Fusion Devices* (CRC Press, 2000).
[11]G. D. Hobbs and J. A. Wesson, Plasma Phys. **9**, 85 (1967).
[12]H. Bruining and J. H. de Boer, Physica **5**, 17 (1938).
[13]M. Ono, M. G. Bell, Y. Hirooka, R. Kaita, H. W. Kugel, G. Mazzitelli, J. E. Menard, S. V. Mirnov, M. Shimada, and C. H. Skinner, Nucl. Fusion **52**, 037001 (2012).
[14]C. H. Skinner, R. Sullenberger, B. E. Koel, M. A. Jaworski, and H. W. Kugel, J. Nucl. Mater. **438**, S647 (2013).
[15]S. Takamura, S. Mizoshita, and N. Ohno, Phys. Plasmas **3**, 4310 (1996).

[16]F. Subba, D. Tskhakaya, H. Burbaumer, U. Holzmuller-Steinacker, N. Schupfer, M. Stanojevic, and S. Kuhn, Plasma Phys. Controlled Fusion **44**, 61 (2002).
[17]Yu. Igitkhanov and G. Janeschitz, J. Nucl. Mater. **290–293**, 99 (2001).
[18]S. Mizoshita, K. Shiraishi, N. Ohno, and S. Takamur, J. Nucl. Mater. **220–222**, 488 (1995).
[19]E. Oyarzabal, A. B. Martín-Rojo, J. A. Ferreira, D. Tafalla, and F. L. Tabares, J. Nucl. Mater. **438**, S792 (2013).
[20]E. Oyarzabal, A. B. Martin-Rojo, and F. L. Tabares, J. Nucl. Mater. **452**, 37 (2014).
[21]See http://www.saesgetters.com for SAES Getters USA, Inc. 1122 East Cheyenne Mountain Blvd., Colorado Springs, CO 80906, USA.
[22]J. Engbaek, G. Nielsen, J. H. Nielsen, and I. Chorkendorff, Surf. Sci. **600**, 1468 (2006).
[23]J. N. Spencer, G. M. Bodner, and L. H. Rickard, *Chemistry: Structure and Dynamics*, 5th ed. (Wiley, 2010).
[24]R. W. G. Wyckoff, *Crystal Structures* (John Wiley, New York, 1963).
[25]R. M. Sullenberger, "Uptake and retention of residual vacuum gases in lithium and lithium films," M.Sc. thesis, Princeton University, 2012.
[26]M. Cao, N. Zhang, T.-C. Hu, F. Wang, and W.-Z. Cui, J. Phys. D: Appl. Phys. **48**, 055501 (2015).
[27]D. Drouin, A. R. Couture, D. Joly, X. Tastet, V. Aimez, and R. Gauvin, Scanning **29**, 92 (2007).
[28]M. I. Patino, Y. Raitses, B. E. Koel, and R. E. Wirz, J. Phys. D: Appl. Phys. **48**, 195204 (2015).
[29]R. Cimino and I. R. Collins, Appl. Surf. Sci. **235**, 231 (2004).
[30]J. M. Pedgley, G. M. McCracken, H. Farhang, and B. H. Blott, J. Nucl. Mater. **198**, 1053 (1992).
[31]R. Mayer and A. Weiss, Phys. Rev. B **38**, 11927 (1988).
[32]V. Viswanathan, K. S. Thygesen, J. S. Hummelshoj, J. K. Norskov, G. Girishkumar, B. D. McCloskey, and A. C. Luntz, J. Chem. Phys. **135**, 214704 (2011).
[33]M. D. Radin and D. J. Siegel, Energy Environ. Sci. **6**, 2370 (2013).
[34]J. R. Hoenigman and R. G. Keil, Appl. Surf. Sci. **18**, 207 (1984).